Los Alamos
NATIONAL LABORATORY

memorandum
Los Alamos Neutron Science Center (LANSCE)
Accelerator Physics and Engineering Group, LANSCE-1

To/MS : Distribution
From/MS : F. Krawczyk, LANSCE-1, MS H817
Phone/FAX/email : 7-1958/5-6590/fkrawczyk@lanl.gov
Symbol : LANSCE-1:TNM-00-076
Date : September 1, 2000

SUBJECT: **Summary of the APT Cavity Data - An Update**

For a consistent use of cavity data throughout the project I summarize all geometry and testing related data that are derived from the rf-simulations for the operating mode of the cavities. This memo supersedes TNM-99-014. Some typing errors are fixed and some information on the evaluation of the rf-measurements for these cavities is added.

This memo consists of four parts:

- **Part 1: The Geometry Data**
- **Part 2: The RF Data**
- **Part 3: Cryo System Support Data**
- **Part 4: Testing Support Data**

Part 1: The Geometry Data

The geometry data are given for 3 different geometries:

- the symmetric structure for β=0.64 with a 6.5 cm radius beam pipe on both sides of the cavity,
- the non-symmetric structure for β=0.64 with a stepped beam pipe on the coupler side of the cavity that achieves the proper external Q-value, and
- the symmetric structure for β=0.82 that is used for the major part of the Accelerator.

The first structure does not have sufficient coupling for the operation in the APT accelerator, but it is still of interest in the context of the summary. It is the basis for the non-symmetric structure at β=0.64, from which it only deviates in the shape of the end cell right at the power coupler. It also represents the geometry of the prototype 5-cell cavities that have been build in Los Alamos and at Grumman.

a. The symmetric structure at β=0.64

This geometry was the basis for the medium energy part of the APT design as described in the final CDR. Some of the cavities that are build and tested within the ED&D program have this geometry. The geometry description is still valid for all β=0.64 half-cells except the one half-cell next to the power couplers.

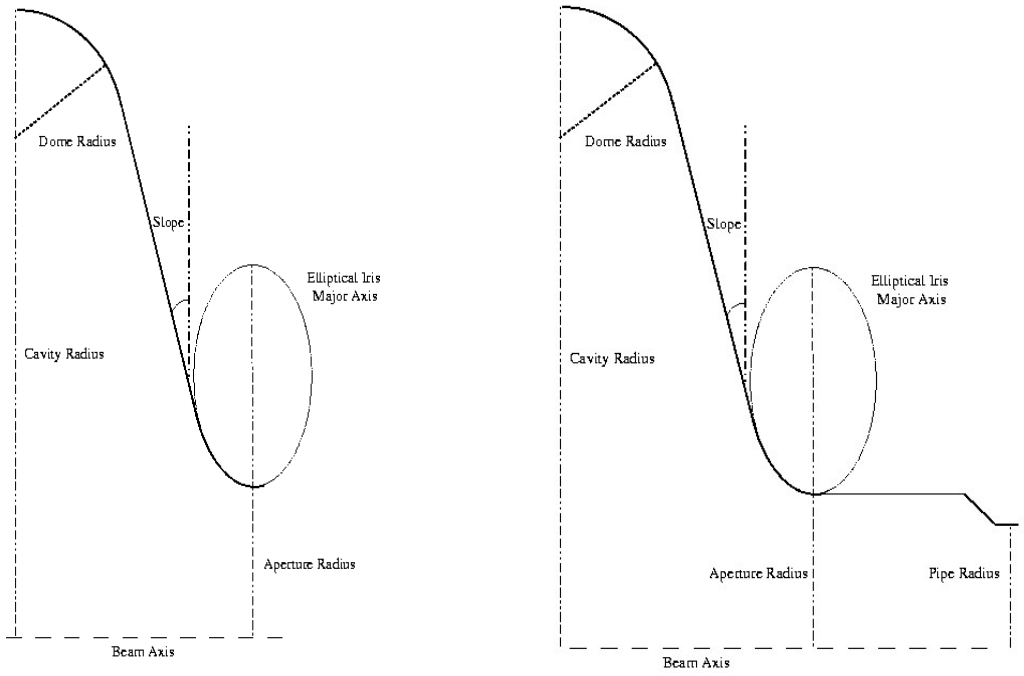

Figure 1: Geometry description for the half-cells of the β=0.64 and 0.82 geometries. The left figure corresponds to all half-cells except for the stepped one used in the non-symmetric β=0.64 structure. The right figure shows the geometry of the stepped half-cell.

Table 1: The Cavity Cell Description for β=0.64

	mid-cell	end-cell
equator coordinate	(19.95,0.0)	(19.95,0.0)
connector	circle, radius=3.233	circle, radius=2.8113
top of straight	(17.278,3.1839)	(17.627,2.7686)
connector	straight, slope 10^o	straight, slope 10^o
bottom of straight	(9.837,4.4960)	(10.505,4.0245)
connector	ellipse, major=10.0	ellipse, major=12.0
iris coordinate	(6.5,6.8537)	(6.5,6.8537)

- the coordinate system for each half-cell uses r=0.0, z=0.0 in the left lower corner,
- the end-cells have inner half-cells that are identical to the mid-cell geometries,
- the elliptical iris region is a segment of an ellipse that has a 2:1 ratio of axes,
- the aperture is 6.5 cm for all half-cells, and
- all lengths are specified in centimeters.

b. The non-symmetric structure at β=0.64

Except for the half-cell next to the power couplers (in the β=0.64 design), this structure is identical to the symmetric β=0.64 cavity structure. The end-cell that is changed (see figure 1) is described as follows:

Table 2: The Cavity Cell Description for β=0.64, "Stepped Beam Pipe" End-Cell

equator coordinate	(19.95,0.0)
connector	circle, radius=3.611
top of straight	(16.966,3.557)
connector	straight, slope 10^o
bottom of straight	(11.237,4.567)
connector	ellipse, major=9.7 cm
iris coordinate	(8.0,6.8537)
connector	straight
end of step	(8.0,21.93491904)
connector	straight
start of beam-pipe	(6.5,24.47491904)

- the coordinate system for each half-cell uses r=0.0, z=0.0 in the left lower corner,
- the elliptical iris region is a segment of an ellipse that has a 2:1 ratio of axes,
- The aperture at the cavity iris is 8.0 cm (the couplers attach to the beam pipe in the 8.0 cm aperture region.). 15.08 cm from the iris it steps down to the nominal 6.5 cm aperture for the rest of the β=0.64 part of the accelerator. The transition is conical with a cone length of 2.54 cm, and
- all lengths are specified in centimeters.

c. The symmetric structure at β=0.82

This structure (see figure 1) is used in the major part of the accelerator. A minor revision might be necessary, if the Q_{ext} is not sufficient. This study has not been done yet.

Table 3: The Cavity Cell Description for β=0.82

	mid-cell	end-cell
equator coordinate	(20.10,0.0)	(20.10,0.0)
connector	circle, radius=4.9685	circle, radius=4.1672
top of straight	(15.9943,4.8930)	(16.6564,4.1039)
connector	straight, slope 10^o	straight, slope 10^o
bottom of straight	(12.6719,5.4788)	(13.940,4.5829)
connector	ellipse, major=14.0	ellipse, major=17.8
iris coordinate	(8.0,8.7796)	(8.0,8.7796)

- the coordinate system for each half-cell uses r=0.0, z=0.0 in the left lower corner,
- the end-cells have inner half-cells that are identical to the mid-cell geometries,
- the elliptical iris region is a segment of an ellipse that has a 2:1 ratio of axes,
- the aperture is 8.0 cm for all half-cells, and
- all lengths are specified in centimeters.

Part 2: The RF-data for the Operating Mode at 700 MHz

The geometries described above were derived in a procedure that optimized (minimized) the peak electric surface fields and provided a mechanically stable structure. Table 4 gives frequencies, field-flatness and cell-to-cell coupling for all geometries.

Table 4: Frequencies, Field Flatness and Coupling

	β=0.64 (symm.)	β=0.64 with step	β=0.82
TM010-0	682.03 MHz	682.08 MHz	674.29 MHz
TM010-1	687.02 MHz	687.11 MHz	681.11 MHz
TM010-2	693.16 MHz	693.24 MHz	689.73 MHz
TM010-3	698.10 MHz	698.05 MHz	696.87 MHz
TM010-π	699.96 MHz	699.90 MHz	699.89 MHz
Coupling	better than 2.6 %	better than 2.6 %	better than 3.7 %
Field Flatness	better than 6.0 %	better than 7.0 %	better than 4.6 %

Take note that the cell-to-cell coupling only regards the next neighbor coupling. Due to the large aperture also second neighbor coupling will contribute and increase the coupling value by a small amount. Also, the nominal frequency of the π-mode is 700 MHz, the frequencies given in the table reflect the simulation accuracy. Finally, the field flatness is the one achieved in the numerical model for the operating mode. In the actual cavity it can be adjusted to the needs of the accelerator. Figures 2-4 (Appendix I) show the accelerating mode and the on-axis longitudinal fields for all three structures.

The next table (Table 5) gives many other important rf-parameters for all three geometries. All these numbers have been derived by simulation of the full 5-cell geometries.

Table 5: RF-Data for the Operating Mode of the 5-cell Cavities

	β=0.64 (symm.)	β=0.64 (with step)	β=0.82	Comment
Q	9.34×10^9	9.40×10^9	12.09×10^9	at $15.9n\Omega$
Geometry Factor	149	149	192	
$T(\beta_{design})$=T_d	0.674	0.650	0.681	
$T_{max}(\beta) = T_{acc}$	0.713	0.699	0.719	
$\beta(T_{acc})$	0.69	0.70	0.89	
Cavity Length	0.6853695	0.6853695	0.877958	m
$E_{acc} = E_0 T_{acc}$	**5.40**	**5.40**	**6.35**	MV/m
E_0	7.57	7.73	8.83	MV/m
$E_0 T_d$	5.11	5.02	6.01	MV/m
E_{peak}	17.66	18.25	18.74	MV/m
H_{peak}	370.5	376.0	422.8	G
Voltage	5.19	5.29	7.75	MV
$E_{peak}/E_0 T_d$	3.47	3.64	3.12	
E_{peak}/E_{acc}	3.27	3.38	2.95	
$H_{peak}/E_0 T_d$	72.66	74.90	66.59	G/MV/m
H_{peak}/E_{acc}	68.62	69.63	63.00	G/MV/m
P_{cav} (Nb)	7.70 W	7.61 W	8.83 W	at $15.9n\Omega$
$P_{cav}(E_{acc} = 1MV/m)$	0.264 W	0.261 W	0.219 W	at $15.9n\Omega$
ZT_{acc}^2/Q	190.13	191.33	290.47	Ω

Note: Where applicable, all numbers are given at the field level of E_{acc} (5.40 MV/m at β=0.64 and 6.35 MV/m at β=0.82).

Important: The Relation Between Field Level and Effective Particle Acceleration

In this paragraph I propose an improved quoting of field levels for specific losses in a cavity. So far there has been a mix-up between field values that represent an actual cavity field level (E_0, E_{acc}) and numbers that indicate the effective acceleration of the beam (E_0T).
The distinction is needed due to the variation of the transit-time factor T with the beam velocity. To keep a prescribed variation or even constant acceleration of the beam (given by E_0T) along the accelerator, the field level (given by E_{acc}) needs to be adjusted. Figure 5 and 6 (Appendix II) show the variation of T with the beam velocity. E_{acc} needs to be adjusted inversely with $T(\beta)$. For the β=0.82 section of the accelerator the value of E_{acc} varies between 5.8 and 6.9 MV/m. All future references for the cavity field level in the APT accelerator should be made with respect to the average field value of **$< \mathbf{E_{acc}} >$=6.35 MV/m.**

The curves in figures 5 and 6 (Appendix II) have been derived by explicit numerical integration, taking into account the field penetration into the pipes and the enlarged pipe-section for the non-symmetric β=0.64 structure. The explicit integration shows that T in an actual structure is slightly lower than in the analytic model (as proposed by Tom Wangler) that disregards the effects of the beam pipe. Also, the β for the maximum T is shifted to a slightly higher value than in the analytical model. Still, the difference between the models is small enough to make them both suitable for the general accelerator layout.

The following table gives the same information as Figures 5 and 6:

Table 6: T Versus Beam Velocity

	β=0.64 (with step)	β=0.64 (symmetric)		β=0.82
β	T(β)	T(β)	β	T(β)
0.50	0.1542	0.1608	0.60	0.0480
0.55	0.3641	0.3889	0.65	0.2065
0.60	0.5485	0.5793	0.70	0.3851
0.62	0.6039	0.6334	0.75	0.5413
0.64	0.6469	0.6735	0.80	0.6515
0.65	0.6632	0.6880	0.82	0.6807
0.67	0.6866	0.7070	0.84	0.7014
0.68	0.6936	0.7116	0.86	0.7142
0.69	0.6977	**0.7132**	0.87	0.7176
0.70	**0.6989**	0.7119	0.88	0.7193
0.71	0.6975	0.7079	0.885	**0.7195**
0.72	0.6935	0.7014	0.89	0.7193
0.74	0.6785	0.6817	0.90	0.7175
0.78	0.6255	0.6204	0.92	0.7095
0.82	0.5504	0.5393	0.95	0.6872
0.90	0.3690	0.3524	0.97	0.6666

Part 3: Data Relevant for the Cryo System Layout

For an estimate of the rf power deposition into the cryogenic load (at 2K) more pessimistic Q-values than the ones given in Table 4 have been used. Table 7 gives Q, surface resistance R_s and power deposition P_{cav} for several scenarios:

1. $R_s = 15.9n\Omega$ is chosen. This surface resistance has been observed in the 805 MHz cavity tested at Los Alamos. For β=0.82 this case corresponds to the results in Table 4 (for β=0.64 Table 4 uses a lower value for E_{acc}).

2. $Q = 5 \times 10^9$ is chosen independent of the geometry factors obtained for the cavities. The "superconducting rf community" suggested this as a reasonably achievable value of Q. This scenario assumes that the surface resistance in the β =0.82 cavities is worse than in the β=0.64 cavities.

3. $Q = 5 \times 10^9$ is used for the β=0.64 cavities and the corresponding surface resistance is used to determine the Q for the β=0.82 structures.

The results in the following table all assume a temperature of 2K and E_{acc}=6.35 MV/m. The input values for each case are printed in bold, the other 2 numbers are calculated with this selection.

Table 7: Rf Losses for Various Q-values

β =**0.64** (symm.)	Case 1	Case 2	Case 3
Q	9.342×10^9	$\mathbf{5.0 \times 10^9}$	$\mathbf{5.0 \times 10^9}$
R_s	**15.9nΩ**	$29.8n\Omega$	$29.8n\Omega$
P_{cav}	10.65 W	19.96 W	19.96 W
β =**0.64** with step			
Q	9.395×10^9	$\mathbf{5.0 \times 10^9}$	$\mathbf{5.0 \times 10^9}$
R_s	**15.9nΩ**	$29.8n\Omega$	$29.8n\Omega$
P_{cav}	10.52 W	19.72 W	19.72 W
$\beta = 0.82$			
Q	12.09×10^9	$\mathbf{5.0 \times 10^9}$	6.44×10^9
R_s	**15.9nΩ**	$38.4n\Omega$	**29.8nΩ**
P_{cav}	8.83 W	21.33 W	16.55 W

The power depositions derived in case 2 are the worst case scenario for nominal cavity performance. The results from case 3 are probably the most reasonable, conservative estimates. A more detailed study of the impact on the cryo system is in progress.

Part 4: Test Support Data

In the last part of this memo I will give the scaling laws and procedures that are useful in the cavity tests. From input power (P_i), reflected power (P_r) and transmitted power (P_t) the values of Q_0 and rf power deposited into the cavity P_{cav} can be determined. These can be used to directly calculate E_{peak}, H_{peak} and E_{acc}. The relations are:

$$E_{peak} = c_1 \times \sqrt{QP_{cav}} \quad [in\ MV/m] \tag{1}$$

$$H_{peak} = c_2 \times \sqrt{QP_{cav}} \quad [in\ G] \tag{2}$$

$$E_{acc} = c_3 \times \sqrt{QP_{cav}} \quad [in\ MV/m] \tag{3}$$

$$E_{peak}/H_{peak} = c_4 \quad [in\ MV/m/G] \tag{4}$$

Table 8 gives all input parameters for the determination of the scaling constants c_1 - c_4, as well as the constants themselves.

Table 8: Scaling Constants for the 5-cell Cavity Tests

	β=0.64 (symm.)	β=0.64 (with step)	β=0.82
Q	9.342×10^9	9.365×10^9	12.09×10^9
P_{cav}	2.682×10^{-14} W	2.608×10^{-14} W	2.695×10^{-14} W
E_{acc}	0.3188 V/m	0.3160 V/m	0.3508 V/m
E_{peak}	1.0431 V/m	1.0684 V/m	1.0352 V/m
H_{peak}	2.1865×10^{-5} G	2.2000×10^{-5} G	2.2100×10^{-5} G
$\sqrt{QP_{cav}}$	0.01583	0.01563	0.01805
c_1	6.5894×10^{-5}	6.8356×10^{-5}	5.7352×10^{-5}
c_2	1.3819×10^{-3}	1.4075×10^{-3}	1.2244×10^{-3}
c_3	2.0139×10^{-5}	2.0218×10^{-5}	1.9435×10^{-5}
c_4	4.768×10^{-2}	4.857×10^{-2}	4.684×10^{-2}

The formulas in Table 9 (next page) give a procedure for the calculation of Q_0, the loaded and external Q's and numbers derived from them. This procedure was suggested by Henri Safa during his sabbatical here in Los Alamos.

The method consists of two steps: The first step is a pulsed measurement to calculate Q_0 directly (from the field decay in the cavity) and some scaling numbers that are related to c_1 - c_4. The second step is a number of cw measurements with increasing field levels in the cavity that give information on the performance of the cavity (e.g. Q vs E_{peak}).

Table 9: Rf Measurement Procedure

- **Pulsed Initialization Measurement**

1. Set drive probe to slightly overcoupled: ($\beta \approx 2.0$)
2. $Q_l = \omega\tau$ ($\tau = t_{1/2}/ln(2)$)
3. CW measurement: Gives P_i, P_r, P_t
4. Calculate α's:
   $\alpha_1 = 0.5 * [1 + \sqrt{P_r/P_i}]$ ($0.5 * [1 - ...]$ if undercoupled)
   $\alpha_2 = 1/(4\alpha_1) * (P_t/P_i)$
   $\alpha_0 = 1 - \alpha_1 - \alpha_2$
5. Calculate reference Q's:
   $Q_1 = Q_{x1} = Q_l/\alpha_1$
   $Q_2 = Q_{x2} = Q_l/\alpha_2$
   $Q_0 = Q_l/\alpha_0$
6. Calculate cavity power: ($P_{cav} = P_i - P_r - P_t$ or $P_{cav} = 4\alpha_0\alpha_1 P_i$)
7. Calculate E_{pk} for CW power level:
   $E_{pk} = (\frac{E_{pk}}{E_{acc}})\frac{\sqrt{ZT^2_{acc}/Q}}{L}(\sqrt{P_{cav}Q_0})$ (with $(\frac{E_{pk}}{E_{acc}})$ and $\sqrt{ZT^2_{acc}/Q}$ from Table 5
   L is the cavity length $(5\frac{\beta\lambda}{2})$ for a 5-cell cavity)
8. calculate k-factor (for E_{pk}): $k = E_{pk}/\sqrt{P_t Q_2}$

Note: The k-factor is identical to c_1 of Table 8

- **CW Measurements**

For each data point:
1. Measure P_i, P_r and P_t
2. Calculate α's (for both over- and undercoupled)
3. Determine coupling from Q-error: (the smaller Q-error determines coupling)
   $Q^-_{err} = \frac{\alpha^-_2 Q_2 - \alpha^-_1 Q_1}{2}$ (if smaller, then undercoupled)
   $Q^+_{err} = \frac{\alpha^+_2 Q_2 + \alpha^+_1 Q_1}{2}$ (if smaller, then overcoupled)
4. $Q_l = \frac{\alpha_1 Q_1 + \alpha_2 Q_2}{2}$
5. $Q_0 = Q_l/\alpha_0$
6. $E_{pk} = k\sqrt{P_t Q_2}$ $(= k\sqrt{P_{cav}Q_0})$
7. $E_{acc} = E_{pk}(\frac{E_{acc}}{E_{pk}})$
8. $B_{pk} = E_{acc}(\frac{B_{pk}}{E_{acc}})$
9. $R_s = G/Q_0$

Conclusion

This document is proposed to be the sole reference for all rf-related cavity data. It should be used throughout all parts of the project. The previous version (TNM-99-014) should not be referenced anymore. In case of any changes further revisions will be distributed by the author.

Appendix I

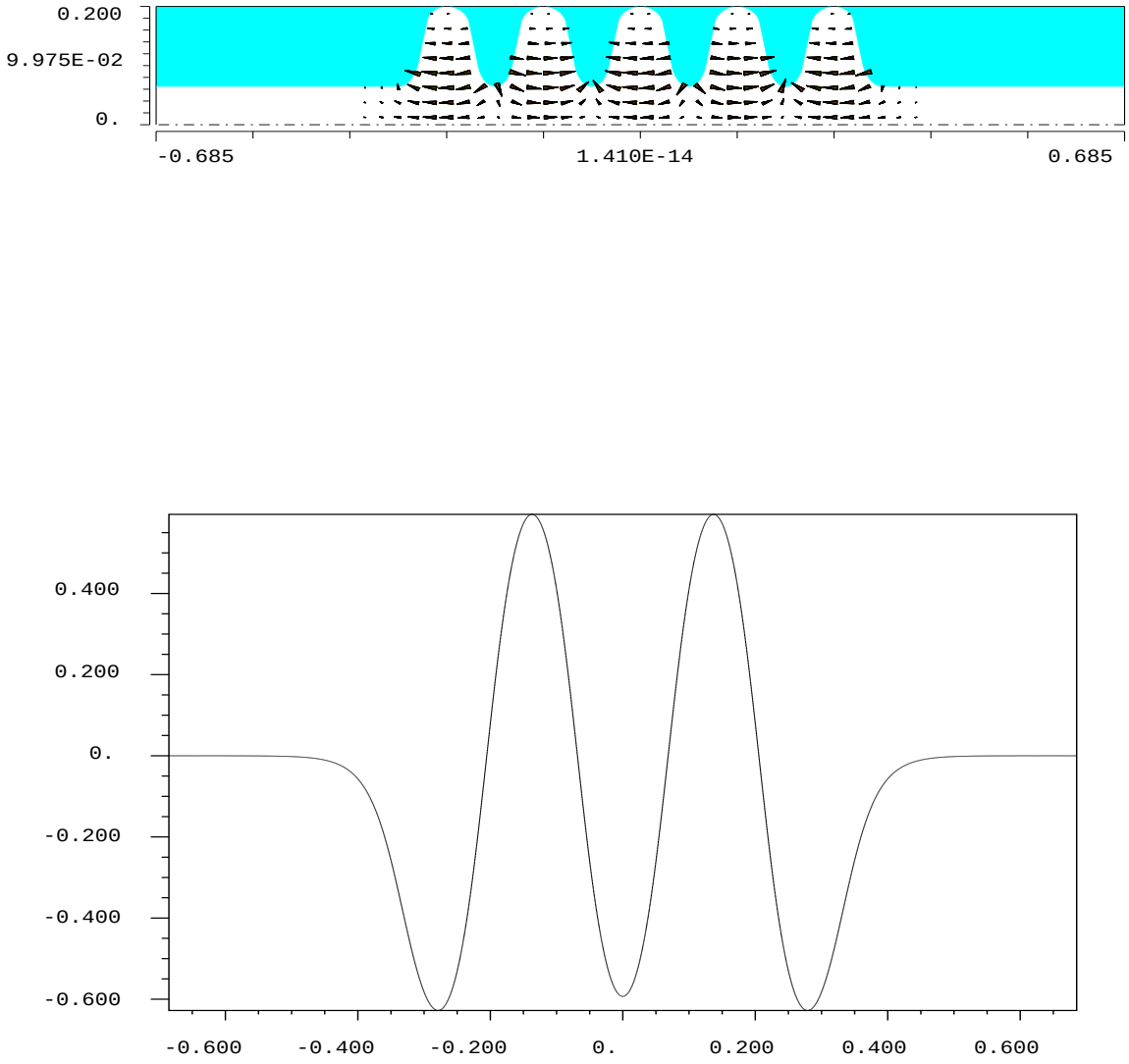

Figure 2: π-mode field pattern and the corresponding on-axis longitudinal field for the symmetric β=0.64 structure.

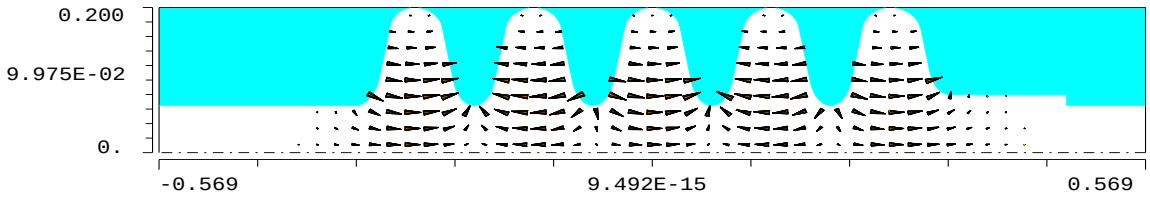

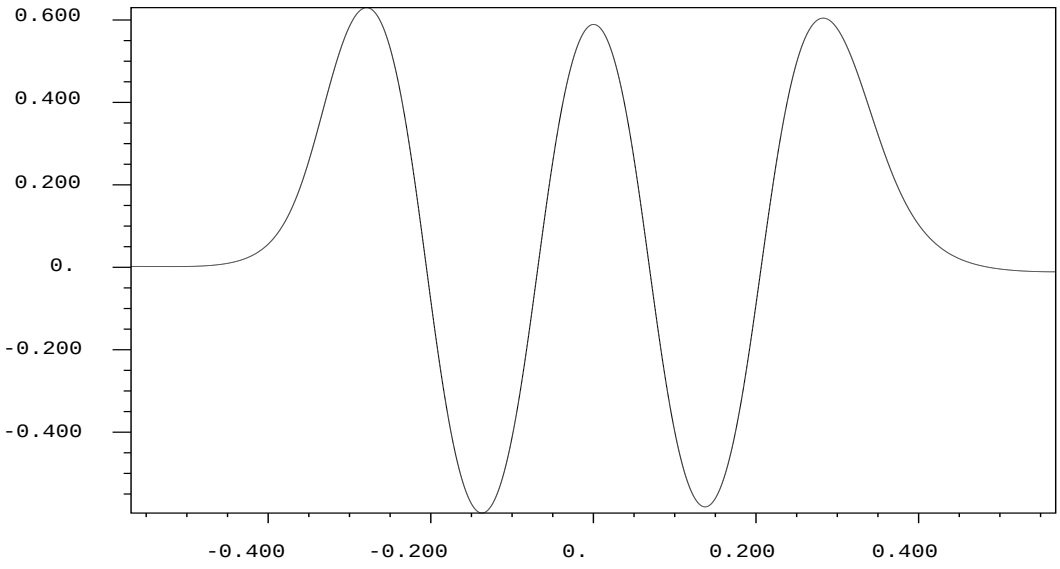

Figure 3: π-mode field pattern and the corresponding on-axis longitudinal field for the β=0.64 structure with the step in the beam pipe.

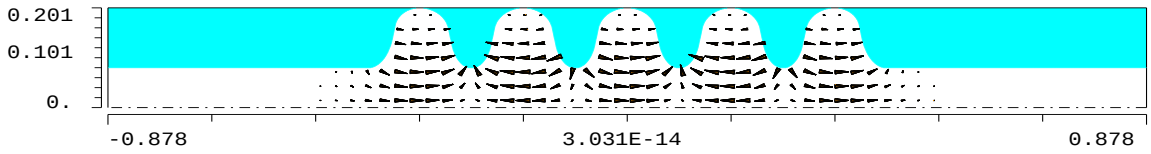

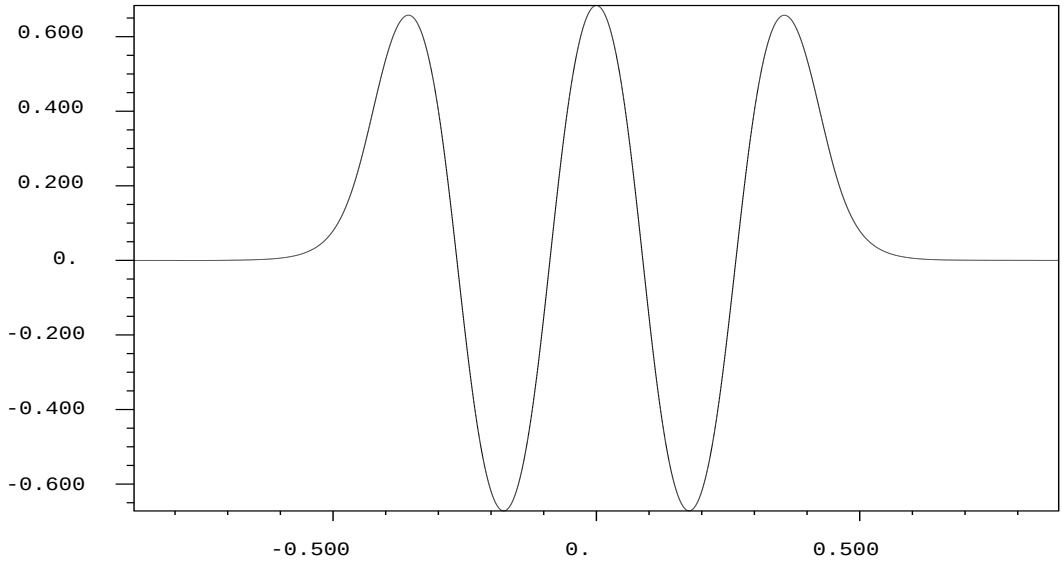

Figure 4: π-mode field pattern and the corresponding on-axis longitudinal field for the β=0.82 structure.

Appendix II

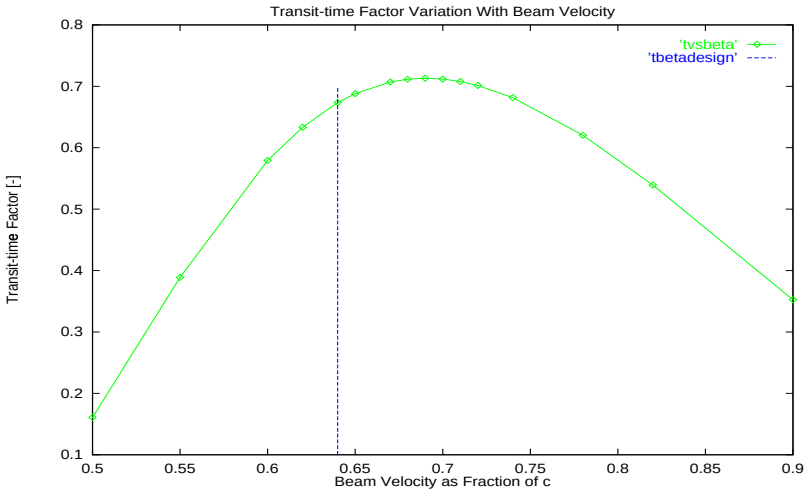

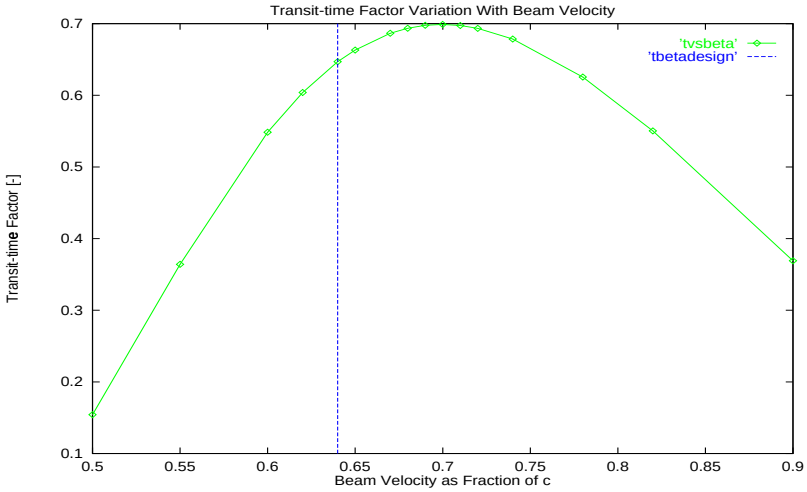

Figure 5: The variation of the transit-time factor with the beam velocity. The plot on the top shows the result for the symmetric at β=0.64, the one at the bottom shows the result for the structure with the stepped beam pipe.

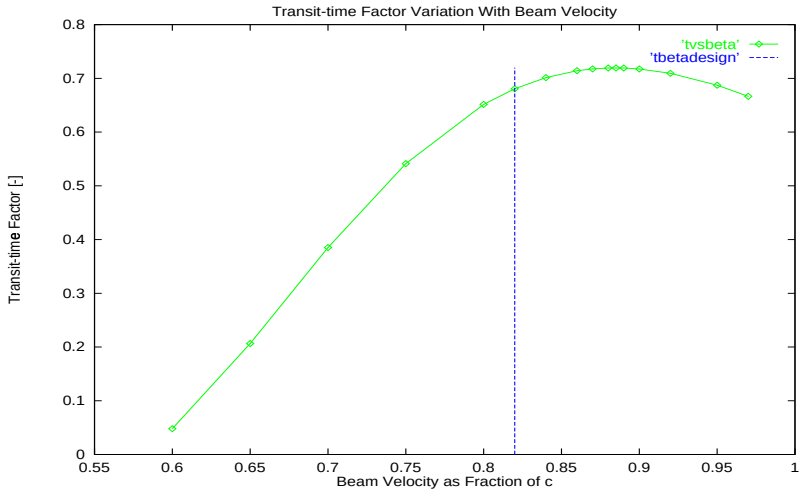

Figure 6: The variation of the transit-time factor with the beam velocity. This plot shows the result for the structure at β=0.82.